Study of Y_1^* Resonant Amplitudes between 1660 and 2215 MeV in the Reaction $K^-N \to \Lambda\pi$†

WESLEY M. SMART*
Lawrence Radiation Laboratory, University of California, Berkeley, California
(Received 25 January 1968)

We have extended the partial-wave analysis of the reaction $K^-N \to \Lambda\pi$ from our data in the energy region 1660 to 1900 MeV to the data at higher energies (1900 to 2215 MeV) from other experiments. This analysis has established the resonant nature of $Y_1^*(1910)$ and measured its spin and parity as $J^P=\frac{5}{2}^+$. The earlier assignment $J^P=\frac{7}{2}^+$ for $Y_1^*(2030)$ by Wohl *et al.* has been confirmed. The mass, width, and $\Lambda\pi$ branching ratio were measured as 1902 ± 11 MeV, 52 ± 25 MeV, and 0.08 ± 0.04 for $Y_1^*(1910)$, and 2032 ± 6 MeV, 160 ± 16 MeV, and 0.41 ± 0.03 for $Y_1^*(2030)$. In addition we found a suggestion for the existence of a $J^P=\frac{1}{2}^+$ resonance at 1880 MeV with a width of 220 MeV.

I. INTRODUCTION

THE study of the reaction $K^-N \to \Lambda\pi$ has proven to be a useful method for learning more about the quantum numbers and resonance parameters of Y_1^* resonances. We have published the results of a partial-wave analysis of this channel, between 1660 and 1900 MeV center-of-mass (c.m.) energy, which yielded information on several Y_1^* resonances.[1] Wohl, Solmitz, and Stevenson identified $Y_1^*(2030)$ from a study of the reaction $K^-p \to \Lambda\pi^0$ between 1900 and 2100 MeV and made the spin-parity assingment $J^P=\frac{7}{2}^+$.[2]

The $I=1$ total KN cross section measured by Cool *et al.*[3] and Davies *et al.*[4] shows a shoulder which is consistent with a resonance at 1910 MeV with a width of 60 MeV. In addition, the $I=1$ total cross section at higher energy shows a peak at 2252 MeV with a width of 200 MeV. Our earlier work[1,5] suggested that the shoulder at 1910 MeV was due to a $J^P=\frac{5}{2}^+$ resonance.

This study, which combines our experimental data (1660 to 1900 MeV) with the data of Wohl *et al.*[2] (1900 to 2100), Trower[6] (1945 MeV), and Dauber[7] (2151 and 2215 MeV), was undertaken primarily to establish the resonant nature of $Y_1^*(1910)$ and to determine its spin-parity assignment. Other goals included: verification of the spin-parity assignment for $Y_1^*(2030)$; measurement of the mass, width, and $\Lambda\pi$ branching ratio for both the $Y_1^*(1910)$ and $Y_1^*(2030)$; possible study of $Y_1^*(2252)$; and determination of the behavior with energy of the nonresonant parts of the partial-wave amplitudes in the $\Lambda\pi$ channel.

This partial-wave analysis of the reaction $K^-N \to \Lambda\pi$ establishes the existence of $Y_1^*(1910)$, determines its spin-parity assignment as $J^P=\frac{5}{2}^+$, and measures its mass, width, and $\Lambda\pi$ branching ratio as $E_R=1902\pm11$ MeV, $\Gamma=52\pm25$ MeV, and $x_{\Lambda\pi}=0.08\pm0.04$. The branching ratio in channel c, x_c is equal to the ratio of the partial width Γ_c in channel c to the total width. In addition, the spin-parity assignment $J^P=\frac{7}{2}^+$ for $Y_1^*(2030)$ is verified and the resonance parameters measured as $E_R=2032\pm6$ MeV, $\Gamma=160\pm16$ MeV, and $x_{\Lambda\pi}=0.41\pm0.03$. No conclusion regarding $Y_1^*(2250)$ could be reached with the available data; however, we find a suggestion for the existence of $Y_1^*(1880)$ with a width of 220 MeV and $J^P=\frac{1}{2}^+$. The nonresonant parts of each of the partial waves up to $G9$ can be adequately described, over the energy region 1660 to 2215 MeV of the data, by no more than six parameters, A, B, C, D, E, and F:

$$T=(A+Bk+Ck^2)e^{i(D+Ek+Fk^2)} \quad \text{if} \quad A+Bk+Ck^2>0, \quad (1a)$$

$$T=0 \quad \text{if} \quad A+Bk+Ck^2<0, \quad (1b)$$

where k is the incoming c.m. momentum.

II. DATA

Table I summarizes the data used in this analysis. The angular distributions and polarizations for the first ten energies listed in the table came from our study of the reaction $K^-n \to \Lambda\pi^-$ in a deuterium bubble chamber.[1,5] The cross sections for these ten energies are twice the cross sections for the reaction $K^-p \to \Lambda\pi^0$, obtained from a companion run with hydrogen in the bubble chamber.[8] Conservation of isotopic spin requires the cross section for $K^-n \to \Lambda\pi^-$ to be twice that for $K^-p \to \Lambda\pi^0$.

The cross sections, angular distributions, and polari-

† Work done under auspices of the U. S. Atomic Energy Commission.
* Present address: Stanford Linear Accelerator Center, Stanford Calif.
[1] W. M. Smart, A. Kernan, G. E. Kalmus, and R. P. Ely, Jr., Phys. Rev. Letters **17**, 556 (1966).
[2] C. G. Wohl, F. T. Solmitz, and M. L. Stevenson, Phys. Rev. Letters **17**, 107 (1966). The data are available from the authors.
[3] R. L. Cool, G. Giacomelli, T. F. Kycia, B. A. Leontic, K. K. Li, A. Lundby, and J. Teiger, Phys. Rev. Letters **16**, 1228 (1966).
[4] J. D. Davies, J. D. Dowell, P. M. Hattersley, R. J. Homer, A. W. O'Dell, A. A. Carter, K. F. Riley, R. J. Tapper, D. V. Bugg, R. S. Gilmore, K. M. Knight, D. C. Salter, G. H. Stafford, and E. J. N. Wilson, Phys. Rev. Letters **18**, 62 (1967).
[5] Wesley M. Smart (Ph.D. thesis), Lawrence Radiation Laboratory Report UCRL-17712, 1967 (unpublished).
[6] W. Peter Trower (Ph.D. thesis), University of Illinois Report COO-1195-54, 1966 (unpublished).
[7] Philip M. Dauber, Ph.D. thesis, Department of Physics, University of California, Los Angles, 1966 (unpublished).
[8] R. W. Birge, R. P. Ely, G. E. Kalmus, J. Louie, A. Kernan, J. S. Sahouria, and W. M. Smart, in *Proceedings of the Second Athens Topical Conference on Resonant Particles, Athens, Ohio, 1965* (University of Ohio, Athens, Ohio, 1965), p. 296; J. Louie (private communication).

TABLE I. Summary of the data used in this analysis.

$E_{c.m.}$ (MeV)	Number of events	Bins in angular distribution	Bins in polarization	Experiment (reference number)	Target
1675	144	9	6	Smart (1,5)	D
1705	394	14	6	Smart (1,5)	D
1730	463	15	6	Smart (1,5)	D
1750	632	19	8	Smart (1,5)	D
1770	626	20	8	Smart (1,5)	D
1790	598	20	9	Smart (1,5)	D
1810	489	17	8	Smart (1,5)	D
1830	496	17	7	Smart (1,5)	D
1855	468	16	7	Smart (1,5)	D
1885	108	7	0	Smart (1,5)	D
1896	719	20	12	Wohl (2)	H
1945	281	15	6	Trower (6)	H
1986	553	20	8	Wohl (2)	H
2026	3412	20	20	Wohl (2)	H
2065	388	20	8	Wohl (2)	H
2109	520	20	8	Wohl (2)	H
2151	394	16	7	Dauber (7)	H
2215	274	15	6	Dauber (7)	H
Total	10959	300	140		

zations at the remaining eight energies came from three studies of $K^-p \to \Lambda\pi^0$ in hydrogen bubble chambers.[2,6,7] The cross sections at these eight energies were also normalized to $K^-n \to \Lambda\pi^-$ (i.e., the $I=1$ cross section). The data were rebinned so as to have at least 10 events or so in each angular distribution bin and 40 events in each polarization bin.

In a bubble-chamber experiment the shape of an angular distribution is determined easily (after correction for biases) from a histogram of the number of events versus the cosine of the c.m. production angle. For measuring a cross section the beam must be normalized, and chamber density, scanning efficiency, and bookkeeping losses determined, etc. Thus the cross-section measurement is open to considerably more errors than the measurement of the angular distribution. If an angular distribution of 20 bins is converted to a differential cross section by using the cross-section measurement, any error in the cross section is introduced into 20 data points, rather than the one data point it actually represents. To avoid this problem we fit the cross sections and the shapes of the angular distributions separately. Because this analysis uses data from four different experiments, this procedure was particularly important.

The angular distributions were expressed as a function of the cosine of the c.m. meson scattering angle $(\hat{K}\cdot\hat{\pi})$; the polarization was calculated from the observed Λ-decay asymmetry relative to the production normal $\hat{n}=\hat{K}\times\hat{\pi}/|\hat{K}\times\hat{\pi}|$, according to the formula $\mathbf{P}_\Lambda\cdot\hat{n}=(3/\alpha_\Lambda)\langle\hat{p}\cdot\hat{n}\rangle$, where $\hat{p}$ is a unit vector parallel to the momentum of the proton in the Λ decay, and α_Λ is 0.66.[9]

[9] A. H. Rosenfeld, A. Barbaro-Galtieri, W. J. Podolsky, L. R. Price, P. Söding, C. G. Wohl, M. Roos, and W. J. Willis, Rev. Mod. Phys. **39**, 1 (1967).

III. THEORY AND FITTING PROCEDURE

The reaction $K^-N \to \Lambda\pi$ is one of a large class called formation experiments, in which a resonant amplitude is excited when the c.m. energy of the K^-N system corresponds to the energy of the resonance. If other amplitudes are small compared to the resonant amplitude, its existence is clearly demonstrated by the rise and fall of the total cross section as a function of energy for the reaction. Unfortunately, in the channel $K^-N \to \Lambda\pi$ the nonresonant amplitudes are not small, and a more detailed examination of the angular distributions and polarizations must be made to determine the mass, width, and branching ratio of the resonance. Also the total cross section gives only a lower limit for the spin and no information on the parity of the resonance.

To obtain the more complete information available in a formation experiment, it is necessary to measure the angular distributions and polarizations of the final baryon in addition to the total reaction cross section, and then decompose the amplitude into partial-wave amplitudes, i.e., eigenstates of angular momentum and parity. A more comprehensive discussion of the theory of partial-wave analysis in formation experiments can be found in an article by Tripp.[10]

In a reaction with spin 0+spin $\frac{1}{2} \to$ spin 0+spin $\frac{1}{2}$ (such as $K^-N \to \Lambda\pi$) the transition operator M is given by

$$M=a(\theta)+b(\theta)\boldsymbol{\sigma}\cdot\hat{n}.$$

There are two amplitudes: a, the non-spin-flip, and b, the spin-flip amplitude. If we define $\hat{K}$ to be a unit vector along the incident K^- c.m. momentum and $\hat{\pi}$ along the final π c.m. momentum, the a and b amplitudes are functions of θ $(\cos\theta=\hat{K}\cdot\hat{\pi})$; $\boldsymbol{\sigma}$ is the Pauli spin operator, and $\hat{n}=(\hat{K}\times\hat{\pi})/(|\hat{K}\times\hat{\pi}|)$ is the normal to the production plane. The relations between $a(\theta)$ and $b(\theta)$ and the complex partial-wave amplitudes $T_l^\pm$ (l is the final orbital angular momentum, $J=l\pm\frac{1}{2}$) are

$$a(\theta)=\lambda\sum_l[(l+1)T_l^+ + lT_l^-]P_l(\cos\theta) \qquad (2a)$$

and

$$b(\theta)=i\lambda\sum_l[T_l^+ - T_l^-]P_l^1(\cos\theta), \qquad (2b)$$

where λ is the incident c.m. wavelength divided by 2π, P_l is the lth-order Legendre polynomial, and $P_l^1(\cos\theta)=\sin\theta dP_l(\cos\theta)/d(\cos\theta)$ is the first associated Legendre polynomial. The differential cross section I and polarization $\mathbf{P}$ are given in terms of a and b by

$$I=d\sigma/d\Omega=|a|^2+|b|^2 \qquad (3a)$$

and

$$I\mathbf{P}=2\,\mathrm{Re}(a^*b)\hat{n}. \qquad (3b)$$

The polarization is restricted to be along $\hat{n}$ by parity conservation in strong interactions. In order to obtain

[10] R. D. Tripp, Ann. Rev. Nucl. Sci. **15**, 325 (1965). The notation in Tripp's article is followed here.

TABLE II. Various notations used for partial-wave amplitudes. The parity P of the two-particle system in the final state has been calculated from $P=(-1)^l P_B P_M=-(-1)^l$ for the usual case of a pseudoscalar meson, M, and even-parity baryon, B.

$T_l^{\pm}$	T_0^+	T_1^-	T_1^+	T_2^-	T_2^+	T_3^-	T_3^+	T_4^-	T_4^+
$l2J$	$S1$	$P1$	$P3$	$D3$	$D5$	$F5$	$F7$	$G7$	$G9$
J^P	$\frac{1}{2}^-$	$\frac{1}{2}^+$	$\frac{3}{2}^+$	$\frac{3}{2}^-$	$\frac{5}{2}^-$	$\frac{5}{2}^+$	$\frac{7}{2}^+$	$\frac{7}{2}^-$	$\frac{9}{2}^-$

a more direct relation between the measured distributions I and $I\mathbf{P}$ and the partial-wave amplitudes, it is customary to make the expansions

$$I=\lambda^2\sum_{m=0} A_m P_m(\cos\theta) \tag{4a}$$

and

$$I\mathbf{P}=\hat{n}\lambda^2\sum_{n=1} B_n P_n{}^1(\cos\theta)\,, \tag{4b}$$

and then refer to tables[10,11] relating the A and B coefficients to the partial-wave amplitude $T^{\pm}$. Table II is useful in converting between the various notations used. The parity P of the two-particle system in the final state has been calculated from $P=(-1)^l P_B P_M=-(-1)^l$ for the usual case of a pseudoscalar meson M and even-parity baryon B.

The variation with c.m. energy of the partial-wave amplitude is, in general, unknown. However, in the special case of a resonant amplitude, it is governed by the Breit-Wigner formula

$$T=\tfrac{1}{2}(\Gamma_e\Gamma_r)^{1/2}/[(E_R-E)-i\Gamma\tfrac{1}{2}], \tag{5}$$

where E is the c.m. energy, E_R the energy of the resonance, Γ_e the partial width in the incident (elastic) channel, Γ_r the partial width in the final (reaction) channel, and $\Gamma=\sum_i\Gamma_i$, where the summation is over all decay channels of the resonance.

A careful study of Eqs. (2) and (3) shows that the transformation $T_l^+\rightarrow T_{l+1}^-$, $T_l^-\rightarrow T_{l-1}^+$ (i.e., changing the parities of all amplitudes) leaves I invariant but changes the sign of $\mathbf{P}$. Also the transformation

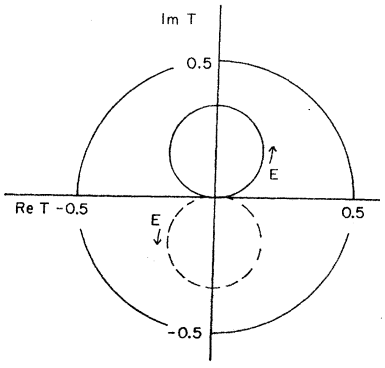

FIG. 1. Argand diagram for a resonant partial-wave amplitude in a reaction channel. The circle at radius 0.5 is the unitary limit.

[11] R. D. Tripp, in *Proceedings of the International School of Physics Enrico Fermi, Varenna, Italy, Course 33* (Academic Press Inc., New York, 1966).

$T_l^{\pm}\rightarrow T_l^{\pm *}$ has the same effect. The first is called the Minami transformation; the second is the complex-conjugation transformation. Measuring the polarization removes two of the four possibilities, but additional information is required to completely specify the solution. Making measurements at several energies and then applying the Wigner condition[11] to a resonant amplitude is sufficient to remove the ambiguity. This condition requires rapidly varying resonant amplitudes to traverse the complex plane in a counterclockwise direction, and is implicit in Eq. (5). Figure 1 is an Argand diagram, which displays the energy behavior of a partial-wave amplitude in the complex plane. Note that there are two possible trajectories for a resonant amplitude, depending on the sign of the numerator in Eq. (5). The choice of trajectories depends on the $SU(3)$ assignment for the resonance and has been discussed previously.[1,5] The circle at radius 0.5 is the unitary limit for partial-wave amplitudes in a reaction channel.

Equations (2) and (3) also show that I and $I\mathbf{P}$ are invariant under the transformation $T_l^{\pm}\rightarrow e^{i\phi}T_l^{\pm}$. In the elastic channel this degeneracy is removed by the optical theorem

$$\mathrm{Im}a(0^\circ)=(k/4\pi)\sigma_T\,, \tag{6}$$

which relates the imaginary part of the forward-scattering amplitude to the total cross section. However, no such relation exists for an inelastic channel, so that the degeneracy is usually taken into account by defining the phase of one of the partial-wave amplitudes.

At one energy there is sufficient information in the experimental distributions I and $I\mathbf{P}$ to just determine all the partial waves (but not to resolve the ambiguity discussed above, or to remove the degeneracy in the inelastic channels). If only the first n partial waves are present, then the expansions (4) require terms up to order $(n-1)$.[10,11] One must determine $2n$ quantities to describe the n complex partial waves. The differential cross section I provides n (A_0, A_1, $\cdots$, A_{n-1}) of these quantities, and the polarization measures $n-1$ (B_1, B_2, $\cdots$, B_{n-1}) more. For the elastic channel the optical theorem provides the remaining relationship to completely determine the n partial waves; for the inelastic channels the one undetermined parameter corresponds to the over-all phase degeneracy. Since precise data, particularly for the polarization, are often not available, one must make assumptions to reduce the number of free parameters to be determined from the data.

The large amount of accurate data in the πN elastic and charge-exchange channels has permitted several authors to publish detailed phase-shift analyses up to c.m. energies of 1600 MeV. These analyses differ basically in the method used to ensure smooth energy dependence of the phase shifts and absorption parameters as a function of c.m. energy in the absence of any

general theory for this dependence. Roper[12] used a power-series expansion in k (the c.m. momenta), plus Breit-Wigner resonance amplitudes. Bransden[13] uses a different parametrization based on dispersion relations and the analytic properties of the partial-wave amplitudes. Bareyre[14] finds a unique solution by fitting data at each energy separately and then selecting the solution that joins smoothly to the lower-energy solution. Auvil[15] and Donnachie[16] require smooth behavior of single-energy solutions plus dispersion-relation calculations for the smaller partial waves.

All these phase-shift analyses used two advantages of the πN elastic problem not available in the inelastic reaction $K^-N \to \Lambda\pi$. The optical theorem [Eq. (6)] removes the phase ambiguity from each energy solution in the elastic channel. To match the phase of solutions at different energies in an inelastic channel requires an assumption for the energy dependence of one partial wave. The πN channels have accurate data for a wide c.m. energy range, from threshold to at least 1600 MeV, permitting a smooth continuation of the less complex low-energy solution to higher energies where $l=3$ or 4 amplitudes are required.

To do a partial-wave analysis on the data of this experiment, the energy behavior of each amplitude was parametrized and then all the data were fitted together. This procedure overcame the two difficulties discussed above and also insured that the Wigner condition was upheld. This was basically Roper's approach,[12] but far fewer parameters for energy dependence were required to adequately fit the $K^-N \to \Lambda\pi$ data.

The partial waves were parametrized by combinations of Breit-Wigner resonances and power-series expansions in k. The resonant part of the amplitudes was given by

$$T=\tfrac{1}{2}e^{i\phi}(\Gamma_e\Gamma_r)^{1/2}/(E_R-E-\tfrac{1}{2}i\Gamma)\,, \qquad (7)$$

where ϕ is the phase angle of the resonant amplitude at resonance energy; for $\phi=0$ the amplitude is pure positive imaginary at resonance. The energy dependence of the partial widths has been approximated as

$$\Gamma_i \propto [k_i^2/(k_i^2+X^2)]^{l_i}k_i/E \qquad (8)$$

by Glashow and Rosenfeld,[17] where X is a mass related to the radius of interaction and k_i and l_i are the momentum and orbital angular momentum of the decay products of the resonance in the ith channel. Glashow and Rosenfeld found $X=350$ MeV from a study of the $SU(3)$ predictions for the partial widths of the $\gamma(J^P=\frac{3}{2}^-)$ octet.[17] Deans and Holladay found that $X=175$ MeV gives a better fit to the $\Delta(1236)$ resonance.[18] Blatt and Weisskopf[19] derive (nonrelativistically) an expression for the energy dependence of Γ_i which is identical in form with Eq. (8) for $l=1$, but differs somewhat for higher l values.

Both the Glashow-Rosenfeld form [Eq. (8)] and the Blatt-Weisskopf form for the energy dependence of Γ were tried in fitting the data. In both cases the best fit was obtained with $X=0$, i.e., a simple k_i/E dependence. The Glashow-Rosenfeld form [Eq. (8)] with with $X=175$ MeV gave an almost identical fit; in view of the work of Deans and Holladay,[18] this form with $X=175$ MeV was used for the results quoted in this article.

The nonresonant part of each partial-wave amplitude was parametrized by

$$T=(A+Bk+Ck^2)e^{i(D+Ek+Fk^2)} \quad \text{if} \quad A+Bk+Ck^2>0\,, \qquad (1a)$$

$$T=0 \quad \text{if} \quad A+Bk+Ck^2<0\,, \qquad (1b)$$

where k is the incident c.m. momentum. The parameters A, B, C, D, E, and F were either varied or set equal to zero. For the resonant part of an amplitude [Eq. (7)], the quantities $(x_e x_r)^{1/2}$ $[=(\Gamma_e\Gamma_r)^{1/2}/\Gamma]$, E_R, Γ, and ϕ were variables. If a particular partial wave contained both a resonant and nonresonant part, Eqs. (1) and (7) were simply added together.

For each fit a hypothesis was made as to which partial waves were resonant [Eq. (7)]. The nonresonant part of each partial wave was approximated by Eq. (1). A set of parameters was chosen to describe each hypothesis and reasonable starting values were guessed for each parameter. These starting values were used to calculate the cross sections, angular distributions, and polarizations. The calculated quantities x_i^c were compared with the observed data points x_i^0 and their errors Δx_i^0 to find χ^2:

$$\chi^2=\sum\left(\frac{x_i^c-x_i^0}{\Delta x_i^0}\right)^2,$$

where the index i runs over all the experimental data points. The χ^2 function was then minimized with respect to all the parameters by the variable metric method[20] using the program VARMIT written at Lawrence Radiation Laboratory by Beals.[21]

[12] L. D. Roper, R. M. Wright, and B. T. Feld, Phys. Rev. **138**, B190 (1965).
[13] B. H. Bransden, R. G. Moorhouse, and P. J. O'Donnell, Phys. Rev. **139**, B1566 (1965); Phys. Letters **19**, 420 (1965).
[14] P. Bareyre, C. Bricman, A. V. Stirling, and G. Villet, Phys. Letters **18**, 342 (1965).
[15] P. Auvil, C. Lovelace, A. Donnachie, and A. T. Lea, Phys. Letters **12**, 76 (1964).
[16] A. Donnachie, R. Kirsopp, A. T. Lea, and C. Lovelace, in *Proceedings of the Thirteenth Annual International Conference on High-Energy Physics, Berkeley, 1966* (University of California Press, Berkeley, 1967), p. 176.
[17] S. L. Glashow and A. H. Rosenfeld, Phys. Rev. Letters **10**, 192 (1963).
[18] S. R. Deans and W. G. Holladay, Bull. Am. Phys. Soc. **11**, 516 (1966).
[19] J. M. Blatt and V. F. Weisskopf, *Theoretical Nuclear Physics* (John Wiley & Sons, New York, 1952), Chap. VIII; also see Ref. 12.
[20] W. C. Davidon, Argonne National Laboratory Report ANL-5990 Rev., 1959 (unpublished).
[21] E. R. Beals, Lawrence Radiation Laboratory, LRL Computer Library Report (unpublished).

VARMIT is a general fitting program for determining the local minimum of a function of many parameters. It requires the calculation of the analytic partial derivatives of the function with respect to each parameter. It then uses an iterative procedure to find a local minimum of the function. At each iteration the minimizing program was supplied with the value of χ^2 and the analytic derivatives of χ^2 with respect to each parameter. These partial derivatives define a gradient direction for the most rapid variation of χ^2. A matrix containing approximate second-partial-derivative information was used to modify the gradient direction. In this modified direction the χ^2 and gradient values of another point were calculated. Then a χ^2 minimum in this direction was found by using a cubic approximation. A quadric approximation to the second derivatives in this direction was used to correct the matrix, and a new iteration was started.

After a satisfactory minimum was obtained, the values of the parameters were displaced randomly from their minimum values, and the above procedure was repeated as a consistency check. Approximately 20 min was required to complete a fit for 50 parameters to 440 data points on the CDC 6600 computer if a reasonable set of starting values was chosen.

After solutions have been obtained for several different parametrizations, the χ^2 values for each can be compared, and parametrizations that do not fit the experimental data can be rejected. This is done by comparing the confidence level,

$$\text{C.L.} \approx (2\pi)^{-1/2}\int_t^\infty e^{-y^2/2}dy; \quad t=(2\chi^2)^{1/2}-(2n-1)^{1/2},$$

which is the probability that another experiment would give a worse fit, assuming that the parametrization accurately describes the actual situation. Here n is the number of degrees of freedom, i.e., the number of independent data points minus the number of free parameters. The equation is valid for $n>30$.

IV. RESULTS OF THE PARTIAL-WAVE ANALYSIS

Figure 2 shows the experimental cross-section points and their errors for $K^-N \to \Lambda\pi$. The curve is calculated from fit number 5, which is described later in this section. The cross sections were plotted in units of $\sigma/4\pi\lambda^2$, λ being the incident K^- c.m. wavelength divided by 2π. These units correspond to A_0, the first coefficient of the Legendre expansion, since integrating the expansion Eq. (4a) over all angles yields

$$\sigma = 4\pi\lambda^2 A_0.$$

The major features of the $K^-N \to \Lambda\pi$ cross section in this energy region are two broad peaks, one centered at 1770 MeV and one at 2025 MeV. The lower bump corresponds to the $Y_1^*(1770)$, $J^P=\frac{5}{2}^-$, and the results

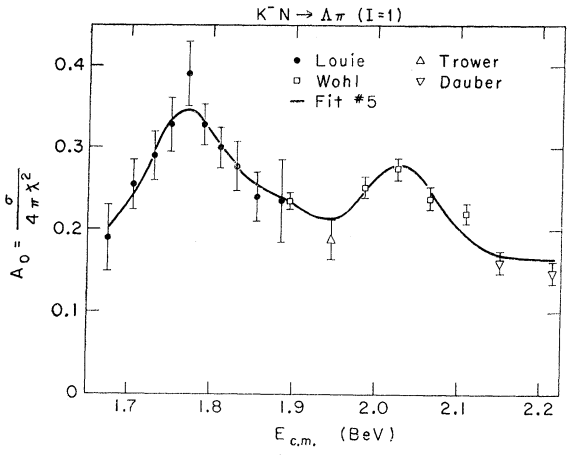

FIG. 2. The $I=1$ total cross section for $K^-N \to \Lambda\pi$, obtained by doubling the cross section measured for $K^-p \to \Lambda\pi^0$. The curve is calculated from fit 5, which was the best fit to the combined data.

of the partial-wave analysis of this energy region have already been published.[1,5] The peak at 2025 MeV corresponds to the $Y_1^*(2030)$, $J^P=\frac{7}{2}^+$, reported by Wohl, Solmitz, and Stevenson.[2]

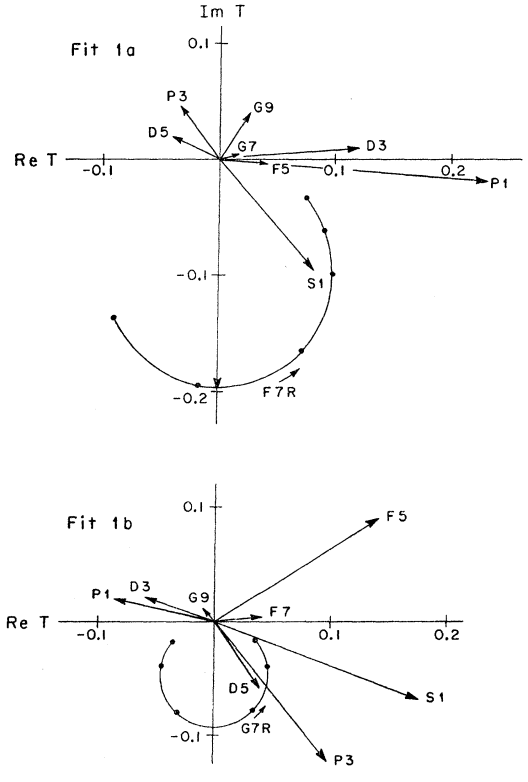

FIG. 3. Argand diagrams for the partial waves (real part versus imaginary part) which best fit the data above 1950 MeV with the hypotheses of constant $S1$, $P1$, $P3$, $D3$, $D5$, $F5$, and $G9$ partial waves plus (a) resonant $F7$ and constant $G7$, and (b) resonant $G7$ and constant $F7$ partial waves. Fit 1a has a confidence level of 0.007; for fit 1b it is 10^{-24}.

TABLE III. Summary of the parametrization used for each partial-wave amplitude used in the fits described in Sec. IV. The number under each amplitude indicates how many parameters [Eq. (1)] were allowed to vary, in the order A, D, B, E, C, F, while the remaining ones were kept fixed at zero. The letter R indicates that a Breit-Wigner resonant amplitude [Eq. (7)] was added to Eq. (1) for that partial wave. The resulting χ^2, number of degrees of freedom (n), and confidence level are also given.

	Amplitudes											
Fit	$S1$	$P1$	$P3$	$D3$	$D5$	$F5$	$F7$	$G7$	$G9$	χ^2	n	C.L.
1*a*	2	2	2	2	2	2	R	2	2	194	149	0.007
1*b*	2	2	2	2	2	2	2	R	2	376	149	10^{-24}
2	6	6	6	6	3+R	6	R	3	3	464	394	0.008
3*a*	6	6	6	6	3+R	4+R	R	3	3	435	394	0.077
3*b*	6	6	4+R	6	3+R	6	R	3	3	472	394	0.004
4	6	6	6	6	3+R	4+R	R	3	3	434	392	0.071
5	6	4+R	6	6	3+R	4+R	R	3	3	418	390	0.161
6	6	4+R	6	6	3+R	6	R	3	3	455	392	0.014
7	6	4+R	6	6	3+R	4+R	R	3	R	429	391	0.089

As a consistency check, the parity assignment for the $Y_1^*(2030)$ was verified in fits 1a and 1b. Only the data for the six highest energies were used, in order to isolate the $Y_1^*(2030)$. In fit 1a a single $\frac{7}{2}^+$ resonant amplitude [Eq. (7)] was hypothesized; in fit 1b a $\frac{7}{2}^-$ resonance was tried instead. In each case the remaining eight partial waves were assumed to be independent of energy; i.e., Eq. (1) with $B=C=E=F=0$ and only A and D variable. In both fits the over-all phase ambiguity was removed by defining $\phi=\pi$ for the $J=\frac{7}{2}$ resonant amplitude. The mass E_R, width Γ, and the magnitude at the resonant energy $(x_{N\bar{K}}x_{\Lambda\pi})^{1/2}$ of the resonant amplitude were also allowed to vary, for a total of 19 parameters.

The solutions that minimize χ^2 for the 1a and 1b hypotheses are shown in Figs. 3(a) and 3(b), and the final χ^2 and confidence levels (C.L.) are listed in Table III. The $J^P=\frac{7}{2}^+$ assignment of Wohl *et al.* for $Y_1^*(2030)$, fit 1a, is seen to make a reasonably good fit to the data, (C.L.$=0.007$) while the alternative $\frac{7}{2}^-$ assignment is totally inadequate to fit the data (C.L.$=10^{-24}$). Both solutions are plotted against the experimental A_i/A_0 and B_i/B_0 coefficients in Fig. 4.

The next step, fit 2, was to attempt to fit all the data at the 18 energies with the well-established $Y_1^*(1770)$, $J^P=\frac{5}{2}^-$, and $Y_1^*(2030)$, $J^P=\frac{7}{2}^+$, resonances plus energy-dependent nonresonant amplitudes. The number of parameters varied in the nonresonant part of each partial-wave amplitude is shown in Table III. All six parameters in Eq. (1) were allowed to vary for the first six partial waves, except for the $D5$ wave—where only A, B, and D were nonzero—in addition to the resonant $Y_1^*(1770)$ amplitude. Only three parameters (A, B, and D) were used for the $G7$ and $G9$ amplitudes, while the $F7$ wave was described entirely by the $Y_1^*(2030)$ amplitude. In this and all remaining fits the over-all phase degeneracy was removed by defining $\phi=0$ for $Y_1^*(1770)$. The partial-wave amplitudes that best fit the data are shown in Fig. 5. The points along the curves correspond to energies at which the experimental data were available (Table I). The χ^2 and confidence level for fit 2 are shown in Table III. The confidence level of 0.8% shows that this fit to the data is not unreasonable.

Since the $I=1$ total cross section shows a shoulder that is consistent with a resonance of mass 1910 MeV and width 50 MeV,[3,4] a resonance of this mass and width was tried in the series of fits 3. This resonance was tried in the $P3$, $D3$, $D5$, $F5$, $F7$, and $G7$ waves; in each case (except $F7$) the number of parameters used to describe the background in that partial wave was reduced, from 6 to 4 ($C=F=0$) or from 3 to 0. The mass and width of the new resonance were held fixed at 1910 and 50 MeV; only the magnitude and ϕ were allowed to vary. The only hypothesis that was an improvement over fit 2 was fit 3a, which establishes the $Y_1^*(1910)$ as $J^P=\frac{5}{2}^+$. The confidence level for fit 3a has increased to 7.7% compared with 0.8% for fit 2. The same number of parameters (six) describing the $F5$ partial wave were allowed to vary in each case. The only change was to allow part of the $F5$ partial wave to come from $Y_1^*(1910)$ in fit 3a. It is easy to see that the complicated energy dependence of the $F5$ wave (Fig. 6) with the $Y_1^*(1910)$ included could not be ob-

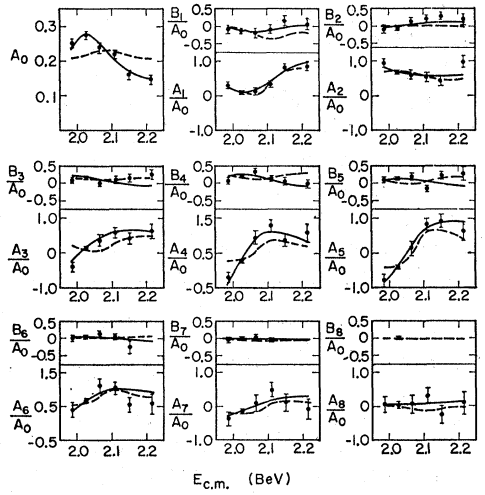

FIG. 4. Comparison of the A_i/A_0 and B_i/A_0 coefficients calculated from fit 1a (solid curve) and 1b (dashed curve) with those obtained from the experimental data.

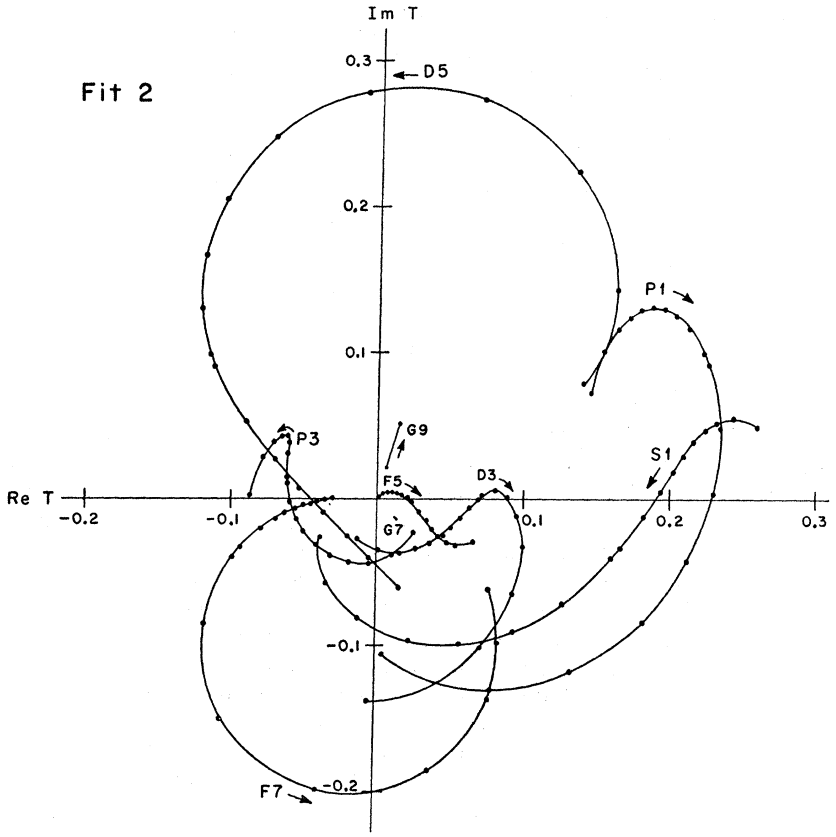

FIG. 5. The partial-wave amplitudes from fit 2 with resonances in the $D5$ and $F7$ waves. The dots indicate the energies at which data were available, as listed in Table I. The solution for the $G7$ wave was essentially constant, even though the parametrization permitted energy variation.

tained with the power-series expansion in k [Eq. (1)] used in fit 2, even though the same number of parameters were allowed to vary in each case. The next most probable fit in the series was 3b, which is for a $\frac{3}{2}^+$ assignment. The confidence level of 0.4% for this fit is less than the 0.8% for fit 2. Fit 3b is included in Table III to show that $J^P=\frac{5}{2}^+$ is the only spin-parity assignment for $Y_1^*(1910)$ allowed by the data.

Fit 4 (Table III) is the same as fit 3a, except that mass and width of the $Y_1^*(1910)$ were allowed to vary as well. The slight decrease in confidence level, from 7.7% in fit 3a to 7.1% in fit 4, indicates that the mass and width for $Y_1^*(1910)$ measured by Cool *et al.*[3] and Davies *et al.*[4] are within errors of the values measured in this analysis.

Fit 2 was found from our earlier fits to the lower ten energies[1,5] by adding the higher-energy data one energy at a time. While doing this we noted the solutions for the $P1$ amplitude went through violent changes as the data from 1900 to 2050 MeV were added. This suggested the possible existence of a resonance in the $P1$ partial wave.

In fit 5 a Breit-Wigner resonance amplitude was added to the $P1$ partial wave and the number of parameters used to describe the nonresonant part of the $P1$ wave was reduced from six to four. The resulting fit has a confidence level of 16.1% and is the best fit to the data, and is shown in Fig. 6. The $P1$ resonance had $(x_e x_r)^{1/2}=0.11\pm0.03$, $E_r=1880\pm40$ MeV, $M=220\pm150$ MeV, and $\phi=27\pm26$ deg. In going from fit 4 to fit 5, two additional parameters were added, and the χ^2 dropped by 16. Clearly the parametrizism of fit 5 is a better approximation to the partial waves; the question is how seriously to take the existence of a $Y_1^*(1880)$ with $J^P=\frac{1}{2}^+$.

Probably the most encouraging fact for the existence of this resonance is that the fitting program could find a χ^2 minimum with reasonable values of $(x_e x_r)^{1/2}$, E_R, Γ, and ϕ. The effect of such a $P1$ resonance on the total KN cross section would be extremely small; assuming the same elasticity as the $Y_1^*(1910)$ one would find the contribution to the cross section only $\frac{1}{3}$ as much and the width four times as broad as the $Y_1^*(1910)$. Another channel, such as $\Sigma\pi$, would be the logical place to look for confirmation of this resonance. This analysis alone can only suggest the existence of $Y_1^*(1880)$, width 220 MeV and $J^P=\frac{1}{2}^+$. The A_i/A_0 and B_i/B_0 coefficients calculated from fit 5 are shown in Fig. 7, plotted against the experimental coefficients.

Fit 6 shows the effect of adding the $P1$ resonance to fit 2, but leaving out the $F5$ $Y_1^*(1910)$ resonance. Fit 7 is the same as fit 5, except that the $G9$ nonresonant amplitude has been replaced by a resonant amplitude with E_R and Γ fixed at 2252 and 200 MeV, corresponding to the $Y_1^*(2250)$ discovered by Cool *et al.* in the K^-N total cross section.[3] The over-all fit to the data is

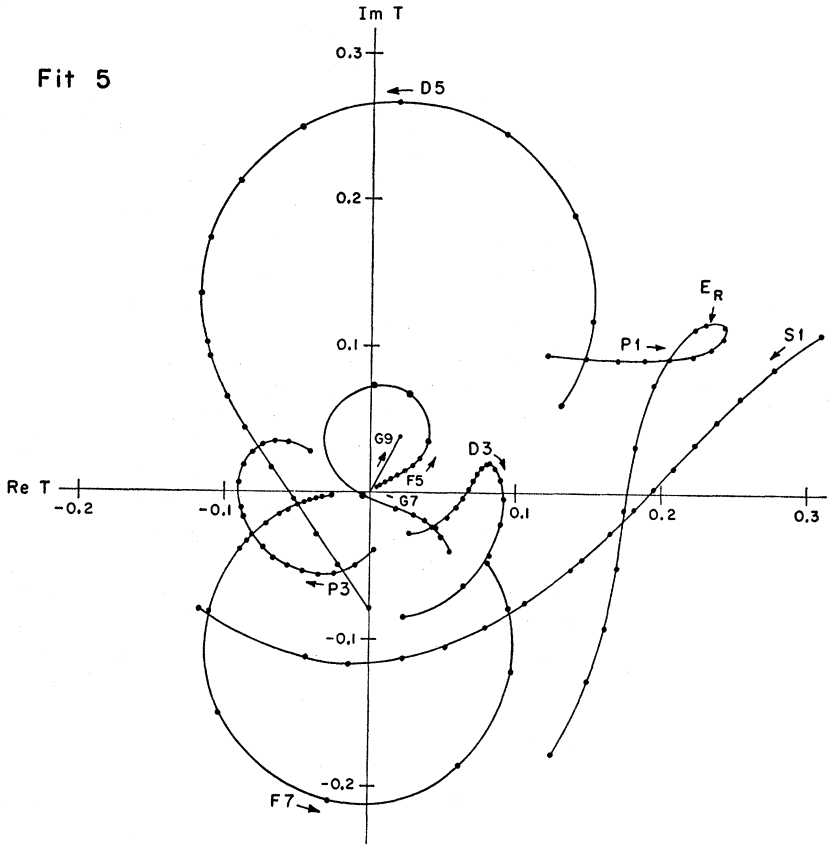

FIG. 6. The partial-wave amplitudes from fit 5 with resonances in the $P1$, $D5$, $F5$, and $F7$ partial waves.

TABLE IV. Parameters and quantum numbers $Y_1^*(1770)$, $Y_1^*(1880)$, $Y_1^*(1910)$, and $Y_1^*(2030)$. The quantities measured or verified in this analysis are italicized; quantities suggested by this analysis are enclosed in parentheses.

Mass E_R (MeV)	Width Γ (MeV)	Spin J	Parity P	$x_{KN}x_{\Lambda\pi}$	$x_{\bar{K}N}$	$x_{\Lambda\pi}$	ϕ (deg)
1775±7	*146±9*	*5/2*	−	*0.071±0.009*	0.45	*0.16±0.02*	0
(1882±40)	(222±150)	(1/2)	(+)	(0.012±0.007)			(−27±26)
1902±11	*52±25*	*5/2*	+	*0.006±0.003*	0.08	*0.08±0.04*	*34±21*
2032±6	*160±16*	*7/2*	+	*0.045±0.004*	0.11	*0.41±0.03*	*174±8*

TABLE V. The A, B, C, D, E, and F parameters [Eq. (1)] determined in fit 5. Only the diagonal elements of the error matrix are quoted for each parameter. However, the form of Eq. (1) introduces large correlations between the parameters. The parameters are given here with sufficient precision to be used to reproduce the partial waves as shown in Fig. 6.

Partial wave	A	B (BeV/c)$^{-1}$	C (BeV/c)$^{-2}$	D (radians)	E (radians) (BeV/c)$^{-1}$	F (radians) (BeV/c)$^{-2}$
$S1$	1.298±0.3	−3.271±1.0	2.263±0.8	−1.81+2.8	11.27± 9.7	−14.69± 8.0
$P1$	−0.008±0.16	0.321±0.3		2.73±0.9	−4.43± 1.3	
$P3$	−0.343+0.3	1.364±1.0	−1.074±0.8	11.17±4.5	−20.19±14.4	11.80±11.2
$D3$	−0.187±0.3	0.758±1.0	−0.514±0.8	−10.74±4.4	36.47±14.5	−30.30±11.7
$D5$	−0.451±0.2	0.683±0.2		5.24±0.2		
$F5$	−0.084±0.04	0.188±0.06		1.74±2.4	−2.74±3.5	
$F7$						
$G7$	0.018±0.03	−0.006±0.04		−0.18±0.35		
$G9$	−0.055±0.02	0.118±0.03				

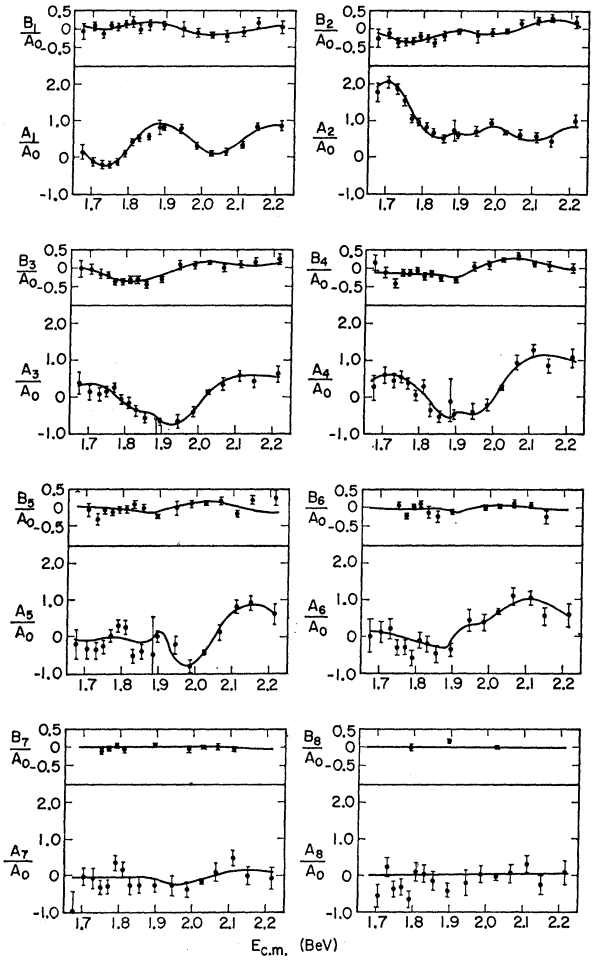

FIG. 7. Comparison of the A_i/A_0 and B_i/A_0 coefficients calculated from fit 5 with those obtained from the experimental data. The values for the cross section (A_0) are shown in Fig. 2.

poorer; any information about $Y_1^*(2250)$ must await data at higher energies and an analysis that includes higher partial waves.

V. CONCLUSIONS

The major result of this analysis was to establish the resonant character of the $Y_1^*(1910)$ reported by Cool *et al.*[3] and to make the spin-parity assignment $J^P=\frac{5}{2}^+$. Other results include: the verification of $J^P=\frac{7}{2}^+$ assignment for $Y_1^*(2030)$ made by Wohl *et al.*[2]; the measurement of the parameters of the Y_1^* resonances in this energy region; the general behavior of the nonresonant partial-wave amplitudes; and the suggestion of a new resonance, $Y_1^*(1880)$ with $J^P=\frac{1}{2}^+$.

Table IV summarizes the parameters of $Y_1^*(1770)$, $Y_1^*(1880)$, $Y_1^*(1910)$, and $Y_1^*(2030)$ determined in fit 5. The quoted errors are the statistical errors calculated in the fitting program, increased by a factor of two. The statistical errors have been doubled in an attempt to include uncertainties arising from the particular parametrization chosen for the nonresonant partial-wave amplitudes and from the somewhat *ad hoc* energy dependence used for Γ in the Breit-Wigner resonance formula. With two exceptions [in fit 2, for $Y_1^*(2030)$, $x_{N\bar{K}}x_{\Lambda\pi}$ was 0.041 (1.1σ) and Γ was 182 MeV (1.5σ)], the corresponding resonance parameters found in fits 2, 3a, 4, 6, and 7 agreed to within the quoted errors of the parameters from fit 5. Since a study of a reaction channel measures only the product of the elastic and reaction branching ratios, $x_{\Lambda\pi}$ has been calculated from the measured product ($x_{N\bar{K}}x_{\Lambda\pi}$) by using the latest world-average values for $x_{N\bar{K}}$.[22]

There is at present no general theory to explain the behavior of nonresonant partial-wave amplitudes. However, this partial-wave analysis yields rough measurements of these amplitudes in the reaction $K^-N\rightarrow\Lambda\pi$. The sum of the nonresonant and any resonant part of each amplitude is shown in Fig. 6 for fit 5. The A, B, C, D, E, and F parameters for this fit are given in Table V. Only the diagonal elements of the error matrix are quoted for each parameter. However, the form of Eq. (1) introduces large correlations between the parameters. The A, B, C, D, E, and F parameters are given in Table V with sufficient precision to enable one to use them to reproduce the partial waves as shown in Fig. 6.

The measurement of ϕ for each resonance yields information on its $SU(3)$ assignment; detailed discussions of this have already been published for $Y_1^*(1770)$, $Y_1^*(1910)$, and $Y_1(2030)$.[5,23] Since $Y_1^*(1880)$ is in phase with $Y^*(1770)$, the restrictions listed in Ref. 23 for $Y_1^*(1770)$ also apply to $Y_1^*(1880)$.

Note added in proof. In the series of fits 3 (see Sec. IV) we have also tried $S1$ and $P1$ assignments for $Y_1^*(1910)$. Neither fit to the data was as good as fit 2. For $S1$, χ^2/n was 469/394 and C.L.$=0.005$; for $P1$, χ^2/n was 467/394 and C.L.$=0.006$.

ACKNOWLEDGMENTS

I wish to thank Professor Robert P. Ely, Jr., for his helpful suggestions and support, and Dr. Anne Kernan and Dr. Charles G. Wohl for their encouragement. I am indebted to Dr. Wohl, Dr. Solmitz, Professor Stevenson, Dr. Trower, and Dr. Dauber for providing their data in a convenient form for this analysis.

[22] A. H. Rosenfeld, N. Barash-Schmidt, A. Barbaro-Galtieri, W. J. Podolsky, L. R. Price, Matts Roos, Paul Söding, W. J. Willis, and C. G. Wohl, Lawrence Radiation Laboratory Report UCRL-8030 (Rev. Sept. 1967) (unpublished).

[23] A. Kernan and W. M. Smart, Phys. Rev. Letters **17**, 832 (1966).